



Titre: Novel cylindrical representation of the STFT for signal analysis
Title:

Auteurs: Jacob Gonzalez-Villagomez, Gonzalez-Villagomez Esau, J. R. René
Authors: Mayer, Carlos Rodríguez-Donate, & Kanglin Xing

Date: 2025

Type: Article de revue / Article

Référence: Gonzalez-Villagomez, J., Esau, G.-V., Mayer, J. R. R., Rodríguez-Donate, C., & Xing, K. (2025). Novel cylindrical representation of the STFT for signal analysis.
Citation: Electronics Letters, 61(1), e70130 (4 pages). <https://doi.org/10.1049/ell2.70130>

Document en libre accès dans PolyPublie

URL de PolyPublie: <https://publications.polymtl.ca/62012/>
PolyPublie URL:

Version: Version officielle de l'éditeur / Published version
Révisé par les pairs / Refereed

Conditions d'utilisation: Creative Commons Attribution 4.0 International (CC BY)
Terms of Use:

Document publié chez l'éditeur officiel


Titre de la revue: Electronics Letters (vol. 61, no. 1)
Journal Title:



Maison d'édition: Wiley
Publisher:



URL officiel: <https://doi.org/10.1049/ell2.70130>
Official URL:

Mention légale: © 2025 The Author(s). Electronics Letters published by John Wiley & Sons Ltd on behalf of The Institution of Engineering and Technology. This is an open access article under the terms of the Creative Commons Attribution License (<http://creativecommons.org/licenses/by/4.0/>), which permits use, distribution and reproduction in any medium, provided the original work is properly cited.
Legal notice:

Novel cylindrical representation of the STFT for signal analysis

Jacob Gonzalez-Villagomez,¹ 

Esau Gonzalez-Villagomez,¹  Rene J. R. Mayer,² 

Carlos Rodriguez-Donate,^{1,✉}  and Kanglin Xing² 

¹Department of Multidisciplinary Studies, University of Guanajuato, Yuriria, Guanajuato, Mexico

²Department of Mechanical Engineering, Polytechnique Montreal, Montreal, Canada

✉ E-mail: c.rodriguezdonate@ugto.mx

The proposal of new signal representation techniques in time-frequency domain can improve the visualization and acquisition of frequency components in various applications. In this sense, this article presents a novel and different representation of the short-time Fourier transform (STFT) spectrogram for signal analysis, based on changing the visualization from a linear to a cylindrical representation by means of a linear transformation. Simulations show that this new representation focuses on the accuracy of the frequency components rather according to the angular position in which they occur; on the other hand it is easier to analyze high-frequency components than those of low frequency. Finally, it is visually easier to identify fixed components along the test in this representation in a wide window STFT analysis.

Introduction: The representation of a signal in different spatial domains is a crucial aspect of the analysis and extraction of harmonic components that alter the signal, which can be attributed to various phenomena. Consequently, the signal can be transformed into different domains and/or representations, which allows the extraction of characteristics that will facilitate and improve the identification of the phenomena being studied. The time, frequency, and time-frequency domains are among the most employed domains for signal analysis. The domains are employed for a plethora of tasks, including the removal of unwanted noise, the identification of harmonics, the reduction of noise, and the design of filters, among others [1].

The fast Fourier transform (FFT) is a widely used technique for decomposing a time-domain signal into the frequency domain [2, 3]. This enables the identification of all the harmonic components it comprises. These characteristics have led to the widespread application of these transforms in a diverse range of fields, including sound and acoustics [4], biomedical engineering [5], communications [6, 7], fault detection [8, 9], and numerous others. Furthermore, if it is necessary to identify when the harmonic components occur, this can be achieved through the short-time Fourier transform (STFT) [10], which provides a representation of the signal in the time-frequency domain. This will also allow identifying harmonics that are shifting over time.

The advantage of utilizing STFT for representing time-frequency signals has opened the way for numerous applications proposed in the literature. In [11] the STFT spectrogram and image processing are used to identify the specific vibration components of rotating machines. In [12], a combination of STFT and local binary pattern (LBP) is proposed to extract features from a set of images and classify them using machine learning. In [13], an energy cumulant of STFT removes the additive white Gaussian noise. In [14], the STFT and finite impulse response filters are used for the real-time detection of arrhythmia. In [15], octonion algebra is employed to develop a novel method for time-frequency representation, namely the octonion short-time Fourier transform (OSTFT). However, as STFT is known to have limitations with respect to its resolution in time and frequency, mainly due to the use of the window size implemented in its computation [16], each of these new representations has its limitations, as well as advantages and disadvantages.

As demonstrated in the current literature, proposing a new signal representation technique in the time-frequency domain can enhance visualization and facilitate the acquisition of frequency components across various applications. This letter proposes a novel and distinctive representation of the STFT spectrogram for signal analysis, based on the

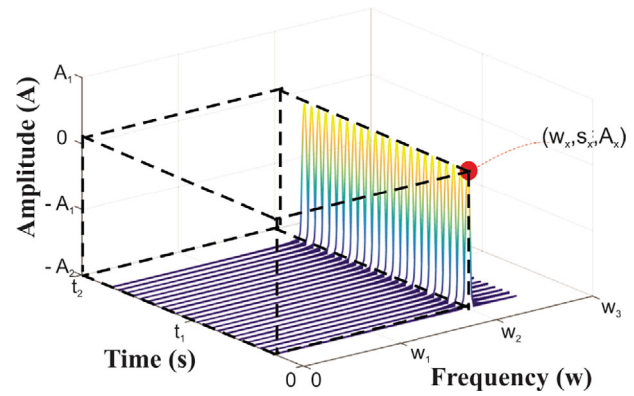


Fig. 1 Displaying a point vector in an R^3 (linear)

transformation of the visualization from a linear to a cylindrical representation through linear transformations. This novel representation is hypothesized to provide significant advantages over the classical linear form. It allows for precise frequency determination based on the angular position of frequency components during cyclic tests. Additionally, it enhances the perception of these components through wide-window analysis of STFT and offers superior frequency image quality, as demonstrated by an improved peak signal-to-noise ratio (PSNR) in the test results.

Graphic representation of the STFT: In order to define the cylindrical transformation of the short Fourier transform spectrogram, various concepts will be addressed to understand this new representation.

Short time Fourier transformation: STFT is based on the discrete Fourier transformation (DFT) that represents the frequency and phase components of a section of a time dependent signal. When dividing the signal into equal sections using windowing techniques by overlapping and performing the DFT, the discrete STFT is obtained, which is described in (1)

$$\text{STFT}x[n](m, \omega) = \sum_{n=-\infty}^{\infty} x[n]w[n-m]e^{-j\omega n}, \quad (1)$$

where $x[n]$ is the time signal to be transferred, n acts as the time step in samples, $w[n-m]$ is the window function which has a smaller duration related to the input signal, m is the length of the window and j is the complex unit. The magnitude squared yields the visual representation of the power spectral density of the function called spectrogram [11].

STFT as a subspace on R^3 : The graphical representation of the STFT is composed of three essential elements: time (s), frequency (ω) and amplitude (A). Due to this, each data obtained from the STFT can be interpreted as a vector in the vector space R^3 of the form as in (2)

$$v = (s, \omega, A), v \in R^3. \quad (2)$$

Therefore, each point of the STFT can be expressed as a three-dimensional element in the vector space R^3 as seen in Figure 1.

Similarly, the data obtained by the STFT as vector points in R^3 allows a linear transformation to be performed to observe the analyzed signal from another perspective without modifying its representative value. Therefore, the graphical display of the Fourier transform representation in cylindrical form is based on a linear transform in the vector space of R^3 , where the linear transform will be defined in (3)

$$T : R^3(\text{linear}) \rightarrow R^3(\text{cylindrical}), \quad (3)$$

and (4)

$$T \begin{pmatrix} \omega \\ s \\ A \end{pmatrix} = \begin{pmatrix} x \\ y \\ A \end{pmatrix}, \quad (4)$$

where x and y are defined in (5) and (6)

$$x = \omega \cos t', \quad (5)$$

$$y = \omega \sin t'. \quad (6)$$

Furthermore, t' is a vector of the angular position of the signal in a movement over time, so it is defined in (7)

$$t' = 0 : \frac{2\pi}{t} : 2\pi, \quad (7)$$

which means that the cylindrical representation of the STFT is defined as a graph that can be visualized as a cycle or revolution.

Demonstration of linear transformation: The linearity of the function defined by (4) is demonstrated under the conditions presented by (8) and (9) defined in [17], which ensure that for each vector in $R^3(\text{linear})$, there is a unique vector in $R^3(\text{cylindrical})$.

$$T(u + v) = T(u) + T(v), \quad (8)$$

$$T(\alpha u) = \alpha T(u), \quad (9)$$

where u and v are vectors of $R^3(\text{linear})$ and α is a scalar. To demonstrate that the linear transform satisfies the condition in (8), two vectors are proposed in $R^3(\text{linear})$ defined by (10) and the transformation defined by (4) is performed.

$$u = \begin{pmatrix} \omega_1 \\ s_1 \\ A_1 \end{pmatrix}, v = \begin{pmatrix} \omega_2 \\ s_2 \\ A_2 \end{pmatrix}, \quad (10)$$

$$\begin{aligned} T(u + v) &= T \begin{pmatrix} \omega_1 + \omega_2 \\ s_1 + s_2 \\ A_1 + A_2 \end{pmatrix} = \begin{pmatrix} x_1 + x_2 \\ y_1 + y_2 \\ A_1 + A_2 \end{pmatrix} \\ &= \begin{pmatrix} \omega_1 \cos t' + \omega_2 \cos t' \\ \omega_1 \sin t' + \omega_2 \sin t' \\ A_1 + A_2 \end{pmatrix} = \begin{pmatrix} (\omega_1 + \omega_2) \cos t' \\ (\omega_1 + \omega_2) \sin t' \\ A_1 + A_2 \end{pmatrix}, \end{aligned} \quad (11)$$

$$T(u) = T \begin{pmatrix} \omega_1 \\ s_1 \\ A_1 \end{pmatrix} = \begin{pmatrix} x_1 \\ y_1 \\ A_1 \end{pmatrix} = \begin{pmatrix} \omega_1 \cos t' \\ \omega_1 \sin t' \\ A_1 \end{pmatrix}, \quad (12)$$

$$T(v) = T \begin{pmatrix} \omega_2 \\ s_2 \\ A_2 \end{pmatrix} = \begin{pmatrix} x_2 \\ y_2 \\ A_2 \end{pmatrix} = \begin{pmatrix} \omega_2 \cos t' \\ \omega_2 \sin t' \\ A_2 \end{pmatrix}, \quad (13)$$

$$\begin{aligned} T(u) + T(v) &= \begin{pmatrix} \omega_1 \cos t' \\ \omega_1 \sin t' \\ A_1 \end{pmatrix} + \begin{pmatrix} \omega_2 \cos t' \\ \omega_2 \sin t' \\ A_2 \end{pmatrix} \\ &= \begin{pmatrix} \omega_1 \cos t' + \omega_2 \cos t' \\ \omega_1 \sin t' + \omega_2 \sin t' \\ A_1 + A_2 \end{pmatrix} = \begin{pmatrix} (\omega_1 + \omega_2) \cos t' \\ (\omega_1 + \omega_2) \sin t' \\ A_1 + A_2 \end{pmatrix}. \end{aligned} \quad (14)$$

When analyzing the result given by (11) and (14), it is observed that it is the same, therefore the transform defined in (4) satisfies the first condition for linearity. On the other hand, for condition in (9) a vector in $R^3(\text{linear})$ and any scalar α is proposed. One of the vectors defined in (10) will be taken, then we have the following proof.

$$T(\alpha u) = T \begin{pmatrix} \alpha \omega_1 \\ \alpha s_1 \\ \alpha A_1 \end{pmatrix} = \begin{pmatrix} \alpha x_1 \\ \alpha y_1 \\ \alpha A_1 \end{pmatrix} = \begin{pmatrix} \alpha \omega_1 \cos t' \\ \alpha \omega_1 \sin t' \\ \alpha A_1 \end{pmatrix}, \quad (15)$$

$$\begin{aligned} \alpha T(u) &= \alpha T \begin{pmatrix} \omega_1 \\ s_1 \\ A_1 \end{pmatrix} = \alpha \begin{pmatrix} x_1 \\ y_1 \\ A_1 \end{pmatrix}, \\ &= \alpha \begin{pmatrix} \omega_1 \cos t' \\ \omega_1 \sin t' \\ A_1 \end{pmatrix} = \begin{pmatrix} \alpha \omega_1 \cos t' \\ \alpha \omega_1 \sin t' \\ \alpha A_1 \end{pmatrix}, \end{aligned} \quad (16)$$

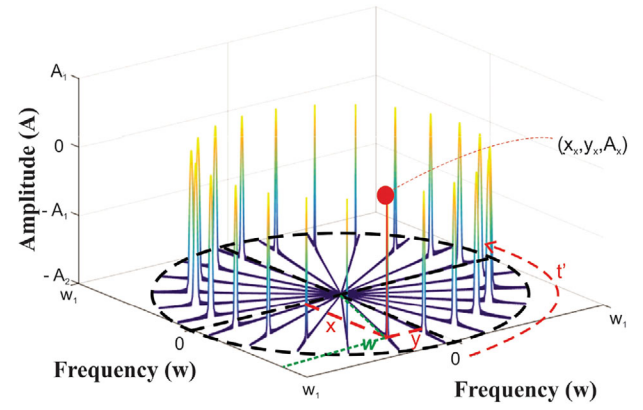


Fig. 2 Displaying a point vector in an $R^3(\text{cylindrical})$

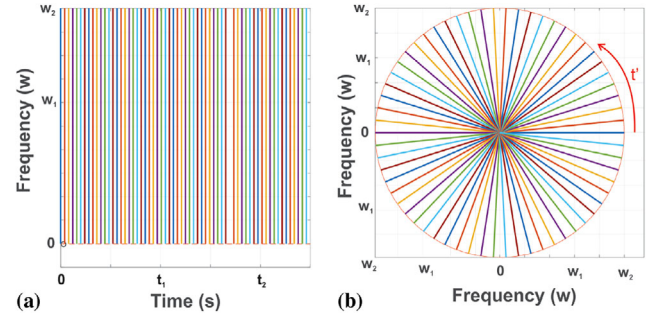


Fig. 3 Comparison of visualization in the time-frequency domain between a) $R^3(\text{linear})$ and b) $R^3(\text{cylindrical})$

where it can be assumed that the second condition for linearity is satisfied since the results in (15) and (16) are the same. In conclusion, within the linear transformation, there is a unique vector as an image in $R^3(\text{cylindrical})$ for each of the vectors in the vector space $R^3(\text{linear})$.

Short Fourier transform in cylindrical shape: Due to the linear transform proposed above, the graphic representation of the STFT in cylindrical form is defined by three elements: x component [ω -angle], y component [ω -angle] and amplitude [A]. Therefore, each data obtained from the STFT in cylindrical form can be interpreted as vectors in the vector space $R^3(\text{cylindrical})$ of the form as in (17).

$$v = (x, y, A), v \in R^3(\text{cylindrical}) \quad (17)$$

Hence, we can express each point of the STFT as a three-dimensional element in the vector space $R^3(\text{cylindrical})$ as seen in Figure 2 where it can be seen that the x and y components will form the frequency perimeter of the vector space $R^3(\text{cylindrical})$, in which the radius will represent the frequency component, while the amplitude (A) will describe the energy density of the spectrogram.

On the other hand, Figure 3 shows a visual comparison of the change in the vector space between $R^3(\text{linear})$ and $R^3(\text{cylindrical})$ from the perspective of the time-frequency plane.

Simulations and results: In order to study the cylindrical representation of the STFT, a synthetic signal was simulated in its linear representation and its representation in cylindrical form. The synthetic signal used is represented by (18),

$$q(t) = \cos(2\pi ft + \phi(t)) + \cos(2\pi f_1 t) + \cos(2\pi f_2 t), \quad (18)$$

where the first term of the equation is the chirp function (signal in which the frequency increases or decreases with time $\phi(t)$ in a range from 0 to 100 Hz), $f_1 = 120$ Hz and $f_2 = 200$ Hz. Furthermore, a Gaussian window was employed for the STFT, with a wide window width (approximately 4000 samples) and a sampling frequency of 1 kHz used to discretise the signal.

The linear representation of the STFT is shown in Figure 4, which depicts the frequency components of the signal described in (18).

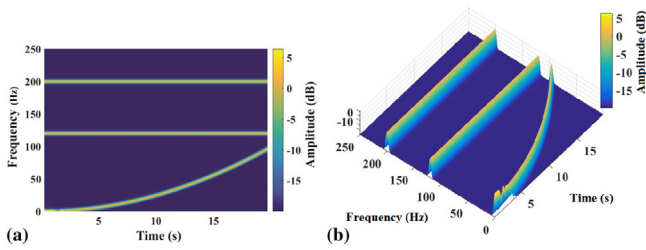


Fig. 4 STFT - $R^3(\text{linear})$ of $x(t)$. (a) Time-frequency plot; (b) three-dimensional plot of the STFT in R^3

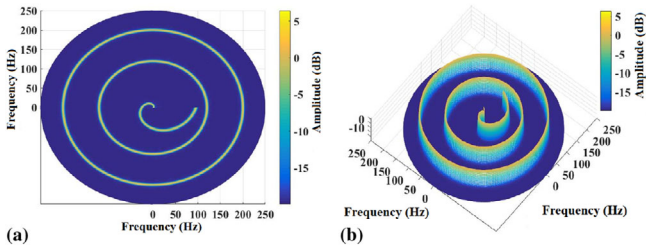


Fig. 5 STFT - $R^3(\text{cylindrical})$ of $x(t)$. (a) Angular momentum-frequency plot; (b) three-dimensional plot of the STFT in R^3

Furthermore, the frequency components of the chirp signal over time are displayed.

Conversely, the cylindrical representation of the signal of (18) is depicted in Figure 5, wherein the frequency components are depicted as circles. This is because the components are found throughout the signal, with the radius representing the frequency value of the signal. Furthermore, the angular position with respect to time is observed to begin in the first quadrant of the signal. This allows the frequency component of the chirp to be monitored as it changes along the signal.

As depicted in Figure 5, the STFT representation is merely a transformation of the original data into a cylindrical format. In this representation, the precision of the frequency components and their angular position are of greater significance.

Discussion: Throughout this paper we have described how to change the perspective of the STFT display to obtain advantages over the classical representation. In order to describe the advantages obtained with the new cylindrical representation of the STFT, a synthetic signal described by (19) is taken and the linear and cylindrical STFTs are shown.

$$q_1(t) = 5 \cos(2\pi f_1 t + \phi_1(t)) + 5 \cos(2\pi f_2 t + \phi_2(t)) + 10VCO \sin(2\pi t) + 2 \sin(2\pi f_2 t) + n(t), \quad (19)$$

where the first two terms of (19) are chirp signals with different frequency changes in the same time, the first from 0 to 500 Hz and the second from 1500 to 2000 Hz. The third term is a representation of a sinusoidal voltage controlled oscillator (VCO). The fourth term is a sinusoidal signal with $f_2 = 850$ Hz and the signal $n(t)$ is a noise signal.

The STFT of $q_1(t)$ in its linear representation is shown in Figure 6, while in its cylindrical representation it is shown in Figure 7.

Due to the visual change of the STFT in its cylindrical form, several advantages can be observed with respect to the classical form, which are: (i) The change of perspective which highlights the approach of having a frequency plane with respect to the angular position that represents the duration of the test in a cycle or revolution; in other words, if the test is circular we can know the angular position where the frequency change occurs. In this example, it can be seen that there is a frequency change approximately at the 45° angular position and that the VCO is repetitive at certain angular position. (ii) In the high frequency analysis, the frequency values of the signal can be observed with greater precision because the values are expanded (like a fan) in this representation; this advantage is better seen in Figure 3. In this case we can see how the high-frequency components of the VCO are appreciated as a zoom. On the other hand, at low frequencies it is difficult to visualise and it

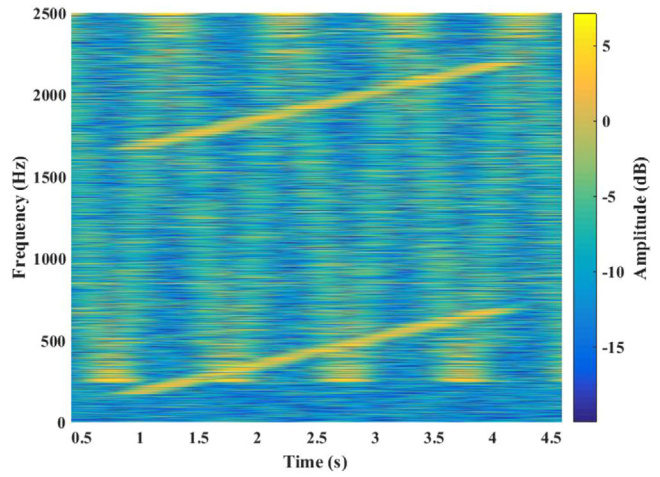


Fig. 6 STFT - $R^3(\text{linear})$ of $x_1(t)$ on time-frequency plot

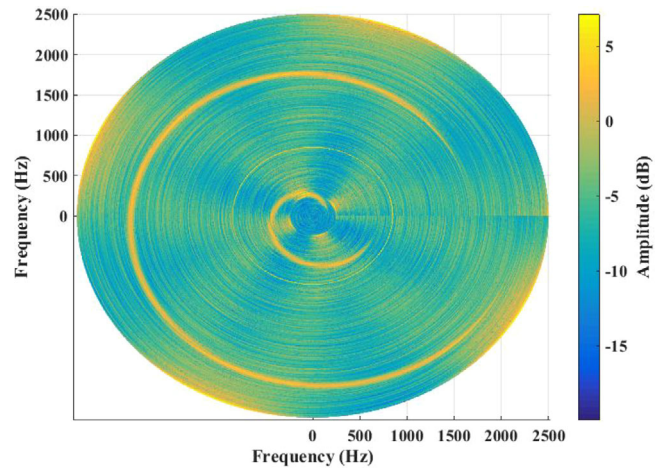


Fig. 7 STFT - $R^3(\text{cylindrical})$ of $x_1(t)$ on angular momentum-Frequency plot

Table 1. Summary of advantages and disadvantages of STFT representations

Representation	STFT linear	STFT cylindrical (proposed)
High frequencies	Equal distribution	Better resolution
Low frequencies	Equal distribution	Lower resolution
Wide window	Loss of frequency components	Noticeable frequency components
Narrow window	Noticeable frequency components	Noticeable frequency components
Particularity	Time and frequency components	Angular position and frequency components
PSNR	23.4870 (low noise), 21.1784 (medium noise), 19.0514 (high noise)	26.5587 (Low noise) 23.7710 (Medium noise) 20.4530 (High noise)

would be necessary to zoom in; this can be seen in the frequency components of the chirp signals. (iii) When using wide windows, where it is desired to know the exact frequency components, the cylindrical STFT is better because the frequency plane is measured in angular positions and not in time, thus highlighting the precision of the frequency components. In addition, the 850 Hz component of $x_1(t)$ is better visualised in the shown representation, since the circle of this frequency is visualised, whereas it is less visible in the classical one. (iv) The peak signal-to-noise ratio (PSNR) is higher in the cylindrical representation of the STFT, which leads to a superior image quality. This analysis is presented in the Table 1, in which different simulations of the signal in 19 were conducted, varying the magnitude of the noise attached to the signal,

and resulting in images of the frequency components. Subsequently, the PSNR was calculated for the image of the signal without noise for each of the STFT representations (linear and cylindrical), thereby obtaining the quantitative value of the signal-to-noise ratio for the representations.

In summary, the cylindrical display focuses on the accuracy of the frequency components according to the angular position in which they occur; on the other hand, it is easier to analyse high frequency components, whereas low frequency components are difficult in this display. Furthermore, the analysis with wide windows of the STFT in the classical form makes it difficult to observe fixed components along the test, while it is easier to identify them visually in the cylindrical form. Finally, the PSNR value in the cylindrical representation is higher, which indicates an enhanced noise performance. The data presented in the Table 1 summarise this conclusion.

Conclusion: This article presents a novel and different representation of the STFT in cylindrical form by a linear transformation. Simulations are used to demonstrate the advantages of this new representation over the classical form. This representation can be used for vibration or frequency analysis of signals acquired in cyclic or circular processes, such as machine tool calibration with the ball bar test, cyclic cutting tests in milling machines and lathe machining, among others. In order to gain further insight into the limitations of this representation and the impact of parameter selectivity on the STFT, experimental tests will be conducted in industrial and calibration processes on future works.

Author contributions: **Jacob Gonzalez-Villagomez:** Conceptualization; formal analysis; investigation; methodology; writing—original draft. **Esau Gonzalez-Villagomez:** Conceptualization; investigation; writing—original draft; writing—review and editing. **Rene J. R. Mayer:** Writing—review and editing. **Carlos Rodriguez-Donate:** Conceptualization; formal analysis; writing—review and editing. **Kanglin Xing:** Writing—review and editing.

Conflict of interest statement: The authors declare no conflicts of interest.

Data availability statement: Data sharing not applicable to this article as no datasets were generated or analysed during the current study

© 2025 The Author(s). *Electronics Letters* published by John Wiley & Sons Ltd on behalf of The Institution of Engineering and Technology.

This is an open access article under the terms of the Creative Commons Attribution License, which permits use, distribution and reproduction in any medium, provided the original work is properly cited.

Received: 9 August 2024 Accepted: 10 December 2024

doi: 10.1049/ell2.70130

References

- 1 Goyal, D., Mongia, C., Sehgal S.: Applications of digital signal processing in monitoring machining processes an rotary components. a review. *IEEE Sens. J.* **21**(7), 8780–8804 (2021)
- 2 Ghani, H.A., Malek, M.R.A., Azmi, M.F.K., Muril, M.J., Azizan, A.: A review on sparse fast fourier transform applications in image processing. *Int. J. Electr. Comput. Eng.* **10**(2), 2088–8708 (2020)
- 3 Lucarini, S., Upadhyay, M.V., Segurado, J.: Fft based approaches in micromechanics: Fundamentals, methods and applications. *Model. Simul. Mat. Sci. Eng.* **30**(2), 023002 (2021)
- 4 Chaki, J.: Pattern analysis based acoustic signal processing: A survey of the state-of-art. *Int. J. Speech Technol.* **24**(4), 913–955 (2021)
- 5 Wu, Y., Ghoraani, B: Biological signal processing and analysis for healthcare monitoring. *Sens.* **22**(14), 5341 (2022)
- 6 Lin, H.-J., Shen, C.-A.: The architectural optimizations of a lowcomplexity and low-latency fft processor for mimo-ofdm communication systems. *J. Signal Process. Syst.* **93**(1), 67–78 (2021)
- 7 Ozkurt, C.: Investigation of the effectiveness of audio processing and filtering strategies in noisy environments on speech recognition performance. *Res. sq.* **1** (2024)
- 8 Abid, A., Khan, M.T., Iqbal, J.: A review on fault detection and diagnosis techniques: Basics and beyond. *Artif. Intell. Rev.* **54**(5), 3639–3664 (2021)
- 9 Tao, H., Wang, P., Chen, Y., Stojanovic, V., Yang, H.: An unsupervised fault diagnosis method for rolling bearing using stft and generative neural networks. *J. Frank. Inst.* **357**(11), 7286–7307 (2020)
- 10 Mateo, C., Talavera, J.A.: Short-time fourier transform with the window size fixed in the frequency domain (stft-fd): Implementation. *SoftwareX* **8**, 5–8 (2018)
- 11 Manhertz, G., Bereczky, A.: Stft spectrogram based hybrid evaluation method for rotating machine transient vibration analysis. *Mech. Syst. Signal Process.* **154**, 107583 (2021)
- 12 Khanna, K., Gambhir, S., Gambhir, M: A novel technique for image classification using short-time fourier transform and local binary pattern. *Multimed. Tools Appl.* **81**(15), 20705–20718 (2022)
- 13 Wang, X., Ying, T., Tian, W.: Spectrum representation based on stft. In: IEEE CISP-BMEI, pp. 435–438. IEEE, Piscataway (2020)
- 14 Farag, M.M.: A self-contained stft cnn for ecg classification and arrhythmia detection at the edge. *IEEE Access* **10**, 94469–94486 (2020)
- 15 Gao, W.-B., Li, B.-Z.: Octonion short-time fourier transform for time-frequency representation and its applications. *IEEE Trans. Signal Process.* **69**, 6386–6398 (2021)
- 16 Mateo, C., Talavera, J.A.: Bridging the gap between the short-time fourier transform (stft), wavelets, the constant-q transform and multi-resolution stft. *Signal, Image and Video P.* **14**(8), 1535–1543 (2020)
- 17 George, R.K., Ajayakumar, A.: A Course in Linear Algebra: Linear transformation, Introduction, Definition 3.1. Springer, Singapore (2024)